RSC Advances

ROYAL SOCIETY OF CHEMISTRY

www.rsc.org/advances

Journal Name

ARTICLE

Hyaluronic Acid-Mediated One-Pot Facile Synthesis of a Sensitive and Biocompatible Gd_2O_3 Nanoprobe for MR Imaging in Vivo

Received 00th January 20xx,
Accepted 00th January 20xx

DOI: 10.1039/x0xx00000x

www.rsc.org/

Haoyu Wang,[a] Yan-Yan Fu,[b] Xuejun Zhang,[b] Chunshui Yu*[a,b] and Shao-Kai Sun*[b]

MR contrast agents play a crucial role in the early diagnosis of various diseases, and plenty of nanoprobes with versatile properties have been developed. However, in order to seek high sensitivity, the biocompatiblity and systemic toxicity assessment of the nanoprobes draw much fewer attention. To meet the requirement in clinic, it is highly desired to develop high sensitive and biocompatible nanoprobe using facile procedure. Herein, we reported a sensitive and biocompatible Gd_2O_3 nanoprobe using hyaluronic acid (HA) via one-pot facile synthesis. HA not only makes the nanoprobe own excellent biocompatibility, but also gives a synergistic effect for improving the sensitivity of the nanoprobe in the aspects of increasing rotational correlation time, water exchange rate and the ratio of surface Gd^{3+} to the inner ones. What's more, the nanoprobe has specific ability for adrenal gland MR imaging. These results suggest that HA-Gd_2O_3 nanoprobe has a promising application prospect in MR imaging in vivo.

Introduction

Magnetic resonance imaging (MRI) as an non-invasive technique plays an important role in the fundamental research and clinical diagnosis, which possesses the merits of high spatial resolution, lack of ionizing radiation, abundant physiological and anatomical information, and remarkable capacity of differentiating soft tissues. To increase the signal contrast between the lesion and normal tissue, MR contrast agent has been widely used in clinical diagnosis.[1, 2] As Gd-based T_1 contrast agents give bright images, which favor the accurate diagnosis of various diseases.[3, 4] Gd-chelates are the most common used T_1-contrast agents in clinic, which own the merits of high thermodynamic and kinetic stabilities, and relatively low toxicity, but suffer from low r_1 values, short blood circulation time, and low specificity to organs or tissues.[3, 4]

With the explosive development of nanotechnology, plenty of nanoprobes with excellent contrast effect, various sizes and shapes, versatile surface modification and long blood circulation have been fabricated to apply in the fields of blood pool imaging, organ and tumor-targeted imaging, highly promoting the early diagnosis of various diseases.[5, 6] To meet the requirement of clinical diagnosis, the security of highly efficient nanoprobe needs to be prior considered for clinical diagnosis.[7, 8] The potential toxicity in vivo seriously limited the further development in the field of translational medicine.[9, 10] The following aspects should be considered for the design of an ideal Gd-based MR contrast: (1) High sensitivity of the contrast agent is essential to distinguish normal and diseased tissues and show significant enhance in enough imaging time. (2) The contrast agent should possess good biocompatibility and show low toxicity in vivo; (3) The developed MR contrast agent should possess a passive or active targeting ability to accumulate in the site of lesion or target organ; (4) Facile synthesis and mild condition are also crucial for the large-scale industrial production.[3] It is very attracting and highly desirable to develop an innovative strategy to fabricate T_1 MRI contrast agents with above-mentioned properties.

To improve the sensitivity of T_1 MRI contrast agent, the parameters that influence relaxivity should be optimized comprehensively.[11] According to the Solomon-Bloembergen-Morgan (SBM) theory,[12] T_1 relaxation originates from the interaction between the surrounding water including inner-sphere, second-sphere and outer-sphere water molecular with the contrast agent.[13] r_1 value is governed by several factors, including the number of inner sphere water molecules (q), rotational tumbling time (τ_R) and water exchange rate (WER).[14] For nanoparticles, water accessible Gd^{3+} ions at the crystal surface play a crucial role in the contribution to longitudinal relaxation of water protons, while bulk Gd^{3+} ions in the crystal lattice don't due to the greatly lowered (or lost) water accessibility of shielded Gd^{3+} ions. The ratio of surface Gd^{3+} to the inner ones (Ratio) could highly influence the relaxivity of nanoprobes.[15, 16] These factors should be considered to develop responsive and high sensitive T_1 contrast agents.

How to improve biocompatibility is attracting more and more attention in the development of nanoprobes for the

[a] Department of Radiology, Tianjin Key Laboratory of Functional Imaging, Tianjin Medical University General Hospital, Tianjin 300052, China.
[b] School of Medical Imaging, Tianjin Medical University, Tianjin 300203, China.
Electronic Supplementary Information (ESI) available: Details of optimization of synthesis condition, XRD and XPS characterization, HE analysis, distribution in major organs in vivo of HA-Gd_2O_3. See DOI: 10.1039/x0xx00000x

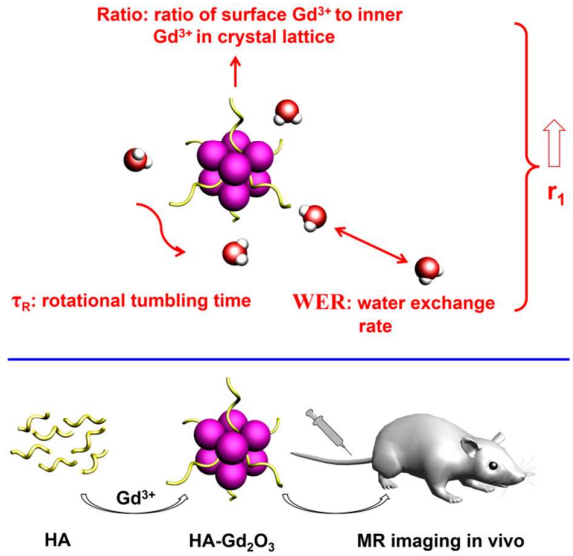

Scheme 1. Schematic Representation of Hyaluronic Acid-Mediated Synthesis of a Gd_2O_3 Nanoprobe for MR Imaging in Vivo.

diagnosis of various diseases.[7-10] Surface modification via biocompatible macromolecules (dextran, chitosan and polyethylene glycol) is the most effective strategy to facilitate the nanoprobe biocompatible.[3, 17] However, the post-modification possesses the disadvantages such as tedious synthesis procedure, aggregation of the nanoparticles and poor water solubility. Recently, mimicking biomineralization processes to fabricate biocompatible nanomaterials using biomacromolecules as template has been extensively investigated. The mild condition and high efficiency make the strategy attractive in the field of nanomedicine.[18] Typically, fluorescent gold nanoclusters,[19] silver nanoclusters,[20] ZnS quantum dot,[21] Gd_2O_3[22] and Gd_2O_3/Au nanoparticles[23] have been synthesized using albumin as template. Special sequence DNA was used to prepare silver nanoclusters with various fluorescent emission wavelength.[24] These nanomaterials as powerful probes have been applied in the field of biosensor and bioimaging.

Base on the theory to enhance T_1 contrast effect and biosynthesis strategy to improve the biocompatibility, we aim to develop a sensitive and biocompatible Gd_2O_3 nanoprobe using hyaluronic acid (HA) via mimicking biomineralization processes. The reasons using HA as the template as follows: First of all, HA is a glycosaminoglycan which distributes widely throughout the body with good biocompatibility and excellent aqueous solubility.[25] In addition, HA-Gd_2O_3 nanoprobe as a slow-tumbling nano-scale contrast agent could increase τ_R and enhance the relaxivity.[12, 14] Last but not least, HA coated on Gd_2O_3 core possesses the strong ability of retaining water molecule, which could increase water exchange rate effectively,[26, 27] and control the growth of Gd_2O_3 crystal with a tiny size, which possess abundant surface Gd^{3+} ions in one nanoparticle, further increase the ratio of surface Gd^{3+} to inner Gd^{3+} ions in crystal lattice.[15, 16] The synergistic effect highly facilitates the sensitivity of the proposed nanoprobe. In general, HA not only makes the nanoprobe own excellent biocompatibility, but also gives a synergistic effect for improving the sensitivity of the nanoprobe.

In our current work, we use HA as a template to load Gd^{3+} and synthesis a highly sensitive HA-Gd_2O_3 nanoprobe with good biocompatibility by a facile one-pot reaction at room temperature successfully. The nanoparticles were characterized with different method and its MR imaging was evaluated in vitro and in vivo compared with Gd-DTPA. This new contrast agent has higher T_1 values and brighter organ contrast enhancement. Moreover, it shows a targeting ability for adrenal gland imaging. The proposed HA-Gd_2O_3 nanoprobe own the merits of high sensitivity, good biocompatibility, low dose in practice, and facile preparation process, which shows great potential in the large-scale industrial production and further application in clinical medicine.

Materials and methods

Materials

HA (sodium salt, Mw ≈ 5000) was purchased from Bloomage Freda Biopharm Co., Ltd. (Jinan, China). $Gd(NO_3)_3 \bullet 6H_2O$ and NaOH were obtained from Aladdin Chemistry Corporation. The deionized water used throughout the experiments was provided by Hangzhou Wahaha Group Co., Ltd. (Hangzhou, China). Cell cultures including RPMI 1640, and fetal calf serum were obtained from Zhaoran Biotechnology Co., Ltd. (Tianjin, China). Kunming mice were purchased from Beijing HFK bioscience Co., Ltd. (Beijing, China) and fed in the SPF animal house. All chemicals and reagents were of analytical grade.

Characterization

The morphology and microstructure were characterized by a Philips Tecnai G2 F20 (Philips, Eindhoven, The Netherlands) field emission high-resolution transmission electron spectroscopy (HRTEM). The samples for HRTEM were prepared by using a 230-mesh Cu grid coated with a lacey carbonfilm and loaded drying sample droplets from water dispersion onto it. The X-ray diffraction (XRD) spectra were collected on a Rigaku D/max-2500 X-ray diffractometer (Rigaku, Tokyo, Japan) with Cu Kα radiation. A Nicolet IR AVATAR-360 spectrometer (Nicolet, USA) with pure KBr as the background were used to measure the Fourier transform infrared (FT-IR) spectra (of 400-4000 cm^{-1}). The measurements of dynamic light scattering (DLS) and zeta potential of HA-Gd_2O_3 nanoprobe were analysed by Malvern Zetasizer Nano ZS model ZEN3600 (standard 633 nm laser, Worcestershire, U.K.).

Synthesis of HA-Gd_2O_3 Nanoprobe

0.2 g of HA was dissolved in 10 mL of water, then 1 ml of $Gd(NO_3)_3 \bullet 6H_2O$ (0.1 M) was added to the above solution under stirring. After 5 mins, 0.6 ml of NaOH (1 M) was added to the mixture to form an alkaline environment (pH ≈ 10). After vigorously stirring for 1 h at room temperature, the solution was dialyzed for 24 h against an excess of water to

remove unreacted reagents, followed by freeze-drying to get the purified product as white flocculent solid.

T_1 relaxivity and T_1-weighted MR imaging in vitro

Different concentrations of HA-Gd_2O_3 nanoprobe and Gd-DTPA were prepared in a series of Gd^{3+} concentration from 0.025 to 1.0 mM in 1.5 mL tubes, respectively. The T_1 relaxivity (r_1) and T_1-weighted MR images of HA-Gd_2O_3 compared with Gd-DTPA were obtained by a 0.5 T MesoMR60 (Shanghai Niumag Corporation, China) with following parameters: multi spin-echo, TR/TE =2000/60 ms, FOV of 100×100 mm, slices=1 and matrix of 192×256.

Stability Measurements

HA-Gd_2O_3 nanoprobe (8 mg/mL) was dissolved in normal saline and stored at 4°C for 1 day and 30 days. Then DLS measurement was carried out to investigate the colloid stability of the nanoprobe.

Cytotoxicity Assay in Vitro

Methyl thiazolyl tetrazolium (MTT) assay is used to assess the in vitro cytotoxicity of nanoprobe. Briefly, a human cervical epidermal carcinoma cell line (HeLa cell) was previously cultured in RPMI-1640 mixed with 10% fetal bovine serum and 1% penicillin–streptomycin. Then the cells were seeded into a 96-well cell culture plate at density of 10000/well. After incubated for 24 h at 37°C under 5% CO_2, different concentration of HA-Gd_2O_3 nanoprobe dissolved in normal saline were added to the wells. The cells were continuous cultured at 37 °C under 5% CO_2. Followed by another 24 h, MTT (10 μL, 5 mg/mL) was added to each well and incubated at 37°C for 4 h. Finally, the upper solution was removed and 120 μL DMSO was added to dissolve the formazan crystal. The optical density was measured at 490 nm by a microplate reader (Bio-tek). The viability of cell growth was calculated by following equation: Cell viability (%) = (mean of sample group/mean of control) × 100%.

Cell uptake in vitro

Cell uptake assay was carried out using HeLa cell, which was seeded into 96-well cellculture plate at density of $5x10^5$/well. Different mass of HA-Gd_2O_3 nanoprobes (25 μg, 125 μg) were added into corresponding wells (n = 6) after incubated for 24 h at 37°C under 5% CO_2. With another 24 h, the extracellular media was removed and the cells were washed with PBS (0.1 mM) twice. These fluid was collected together as extracellular medium. Then the cells were digested by pancreatin cas and also washed with PBS twice to obtain intracellular fluid. The collected fluid was all dissolved by aqua regia and quantified through ICP-MS to assess the percentage of Gd element by cell uptake.

Biodistribution of the nanoprobe

To assess tissue distribution of HA-Gd_2O_3 nanoprobe, the Kunming mice were treated with HA-Gd_2O_3 (0.025 mmol Gd/kg). Then the mice were sacrificed and the major organs (heart, liver, spleen, lung, kidney and adrenal gland) were collected at various times (2 days, 15 days, 30 days, n = 3 for each time point). These organs were dissolved by aqua regia for a week and then the Gd contents were analysed by ICP-MS.

Toxicity assay in vivo

All the animal studies were conducted with the approval of the Tianjin Medical University Animal Care and Use Committee. Kunming mice (24~26 g) and HA-Gd_2O_3 nanoprobe dissolved in normal saline were prepared for assay. (a) Weight change: Kunming mice with intravenous injection of 0.2 mL HA-Gd_2O_3 saline solution (0.025 mmol Gd/kg) and normal saline were regarded as the test and control group, respectively (n = 3 for each group). The body weight were monitored for a month. (b) Histology Analysis: After intravenous injection of HA-Gd_2O_3 (200 μL, 0.025 mmol Gd/kg) as test group and normal saline (200 μL) as control group, the mice were sacrificed at different time points (1, 7 and 30 days) and the major organs (including heat, liver, spleen, kidney and adrenal gland) were extracted. These organs were kept in formaldehyde (4%) and stained with hematoxylin and eosin (H&E) to investigate the histological toxicity of the nanoprobe. (c) Blood biochemistry assessment: Blood samples were harvested from mice treated with HA-Gd_2O_3 (200 μL, 0.025 mmol Gd/kg) as test group and without injection as control group (n = 3 for each group) at different time (1 and 7 days). Liver function markers including total protein (TP), albumin (ALB), globulin (GLB), alanine aminotransferase (ALT), gamma glutamyl transaminase (GGT), aspartate aminotransferase (AST), and kidney function indicators including urea (UREA) and creatinine (CREA)) were analyzed in clinical laboratory in Tianjin Medical University General Hospital.

MR imaging in vivo

MR imaging of mice before and after intravenous injection of 200 μL of HA-Gd_2O_3 (0.025 mmol Gd/kg), Gd-DTPA (0.025 mmol Gd/kg) and Gd-DTPA (0.1 mmol Gd/kg), respectively, was performed on a 3.0 T clinical MR system with a small animal receiver coil (GE Signa Excite). The mice were anesthetized by 4% chloral hydrate (6 mL/kg) and MR Images were obtained with a series of time post injection of contrast agents using a fast spin-echo sequence with the following parameters: (TR/TE = 360/10 ms; FA = 111°; FOV = 100 mm × 100 mm; slice thickness = 3 mm without gap; 7 coronal slices obtained).

Results and Discussion

Synthesis and characterizations

To obtain a HA-Gd_2O_3 nanoprobe with high Gd content and good colloid stability, the dosage of Gd^{3+} was carefully optimized. Typically, 1 ml of different concentrations of $Gd(NO_3)_3$ (0.02 M, 0.05 M 0.1 M, 0.2 M, 0.5 M) was added respectively to 10 ml of HA aqueous solution (20 mg/ml) and then NaOH was introduced to proceed the reaction in an alkaline environment (pH ≈ 10). As show in Fig. S1, the precipitation began to arise as the concentration of Gd^{3+}

increased to 0.2 M, which indicated HA could not stabilize the Gd_2O_3 nanoparticles efficiently. So 0.1 M was chosen to be the optimal reaction concentration to meet requirements in the aspects of high Gd content and good colloid stability.

The prepared HA-Gd_2O_3 nanoprobe was characterized by HRTEM, DLS, FL-IR, XRD and XPS. HRTEM showed the morphological shape of nanoprobe was spherical and the mean diameter was about 2 nm (Fig. 1a; Fig. S2). As strong hydrogen bond formation occurred between water molecules and adjacent carboxyl and N-acetyl groups of HA, the hydrodynamic diameter origined from assembly nanoprobes was much larger than particle diameter (2 nm) estimated from HRTEM.[28] The zeta potential of nanoprobe dispersed in water is -15.5 mV. The FT-IR spectra showed that the characteristic bands of pure HA exhibited O-H stretching at 3200-3500 cm^{-1}, a shoulder peak at around 2900 cm^{-1} associated with $–CH_2$, the peak at 1407 cm^{-1} and 1616 cm^{-1} related to C=O and CO-NH (amide) respectively. The HA-Gd_2O_3 nanoprobe also exhibited the same typical peaks as pure HA, which demonstrated the presence of HA in the prepared nanoprobe (Fig. 1b).[29, 30] As shown in Fig. S3, the typical 222 peak of Gd_2O_3 could be seen in XRD pattern of the nanoprobe.[31] To further investigate the oxidation state of Gd, XPS analysis was performed. As shown in Fig. S4, Gd 4d spectrum was deconvoluted into two components, which was assigned to Gd $4d_{3/2}$ and Gd $4d_{5/2}$ in Gd_2O_3,[32, 33] respectively.

Stability Measurements

The stability of the nanoprobe was estimated by DSL measurement, the result showed the hydrodynamic diameter of HA-Gd_2O_3 dispersed in normal saline for 30 days had no notable difference to that of the nanoparticles stored for 1 day (Fig. S5). The above experimental results indicated the nanoprobe possessed good colloidal stability in saline solution, which could be used for the further study in biological applications.

T_1 relaxivity and T_1-weighted MR imaging in vitro

The T_1 relaxivity characterization and in vitro MR imaging of the nanoprobe and Gd-DTPA were performed on a 0.5 T MR scanner. The r_1 value of the contrast agents were calculated through the measurement of T_1 value as a function of Gd^{3+} concentration. As shown in Fig. 2a, HA-Gd_2O_3 nanorobe showed a high r_1 value of 14.95 $mM^{-1}s^{-1}$, which was almost three times higher than that of Gd-DTPA (5.02 $mM^{-1}s^{-1}$). In addition, compared to Gd-DTPA, HA-Gd_2O_3 shows obviously brighter T_1- weighted MR images even with much lower

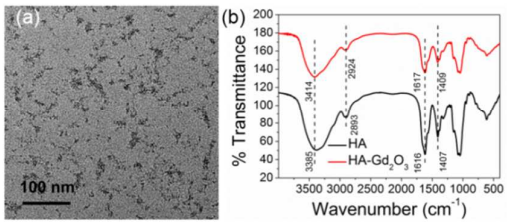

Fig. 1 (a) HRTEM of HA-Gd_2O_3 nanoprobe. (b) FT-IR spectra of HA and HA-Gd_2O_3 nanoprobe.

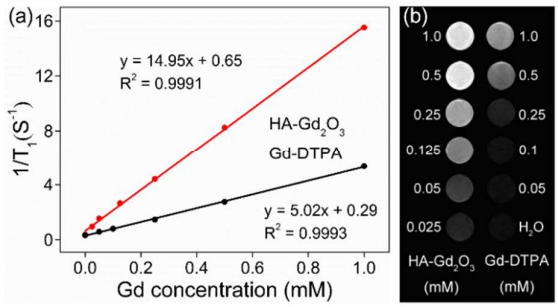

Fig. 2 (a) r_1 relaxivity curves of HA-Gd_2O_3 nanoprobe; (b) T_1 MR imaging in vitro of Gd-DTPA and HA-Gd_2O_3 nanoprobe at various Gd concentration.

concentration of Gd^{3+} (Fig. 2b).

The above results clearly indicated the proposed HA-Gd_2O_3 nanprobe possess much higher sensitivity than the commercial Gd-DTPA agent. The results could be explained as follows: (1) Compared to the small Gd^{3+} chelates with low relaxivity derived from rapid tumbling,[12] HA-Gd_2O_3 nanoprobe with the nanoscale size had much slower tumbling, which resulted in a more efficient relaxation mechanism of the bound water.[12] (2) HA could control the growth of Gd_2O_3 with a tiny size and increase the ratio of surface Gd^{3+} to inner Gd^{3+} ions in crystal lattice, enabling major Gd^{3+} could interact with water molecule.[15, 16] (3) Hydrogen bond formation between water molecules and adjacent carboxyl and N-acetyl of HA leads to the unique water retention capacity of the polymer,[28] and the increased the local water density could improve the water exchange rate,[26, 27] leading to high T_1 relaxivity. The synergistic effects insured the high r_1 value of HA-Gd_2O_3 nanoprobe.

In vitro cytotoxicity assay

In vitro cytotoxicity of HA-Gd_2O_3 nanoprobe was investigated before the biological application. MTT assay was carried out to assess the HeLa cell viability after exposed to different concentrations of HA-Gd_2O_3 nanoprobe for 24 h (Fig. 3a). The nanoprobe showed negligible cytotoxicity even when the concentration was as high as 1 mg/mL, which was much higher than those in most of the previous reports of Gd-based nanoprobes. The cell uptake assay showed a small part of the nanoprobe was internalized by HeLa cells (Fig. S6). Therefore, these results demonstrated that the HA-Gd_2O_3 nanoprobe

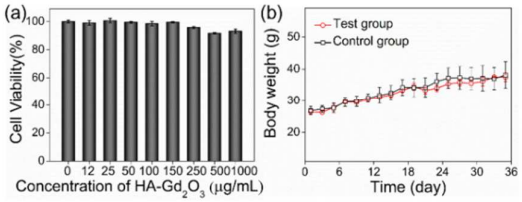

Fig. 3 (a) MTT assay of HeLa cells viability after treatment with various concentration of HA-Gd_2O_3 nanoprobe for 24 h. (b) Body weight change of test group and control group mice for a month.

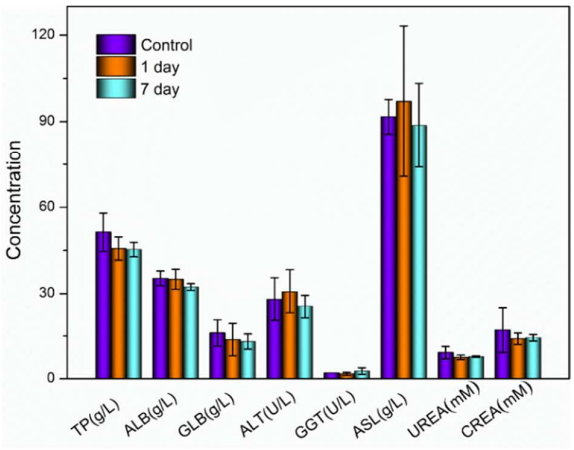

Fig. 4 Blood biochemistry assessment of the mice after treatment with and without HA-Gd_2O_3 nanoprobe (200 µl, 0.025 mmol Gd/kg) at 1 and 7 days (n=3).

possessed negligible cytotoxicity and an excellent biocompatibility.

Toxicity assay in vivo

Biodistribution study, body weight monitoring and histological changes of major organs were carried out to further investigate acute and long-term toxicity of HA-Gd_2O_3 nanoprobe in vivo. The biodistribution of the HA-Gd_2O_3 nanoprobe in different organs were determinated. The results indicated the nanoprobe was mainly accumulated in spleen and liver, a few nanoprobe found in kidney, and the nanoprobe was gradually metabolized with time (Fig. S7). According to the previous study, Gd_2O_3 nanoprobe probably decomposed in the lysosomes where the pH value is about 4.5 after endocytosis by the cells, and excreted out from the body gradually.[34] As shown in Fig. 3b, there was no significant difference between the test group and control group. In addition, compared with control group, the test group also showed normal physical behaviors during experiment. To estimate whether the nanoprobe could cause any histopathological damages, major organs (heat, liver, spleen, kidney and adrenal gland) of the mice were extracted at different time points post-injection of the nanoprobe and analyzed by H&E staining. The results, as shown in Fig. S8, displayed no obvious lesions in test group and their histomorphology showed no difference compared to control group.

Furthermore, blood biochemistry analysis was also performed to assess the potential toxicity in mice at different time points post injection of the nanoprobe. Several indicators were analyzed to reflect the hepatic and kidney function. As shown in Fig. 4, liver function indicators (TP, ALB, GLB, ALT, GGT and ASL) and kidney function indicators (UREA and CREA) of test group were all measured to be normal. The results indicated the nanoprobe had no notable toxicity to the function of hepatic and kidney. In view of the toxicity assay above, HA-Gd_2O_3 nanoprobe exhibited high biocompatibility in vivo and could be use d for the further MR imaging in vivo.

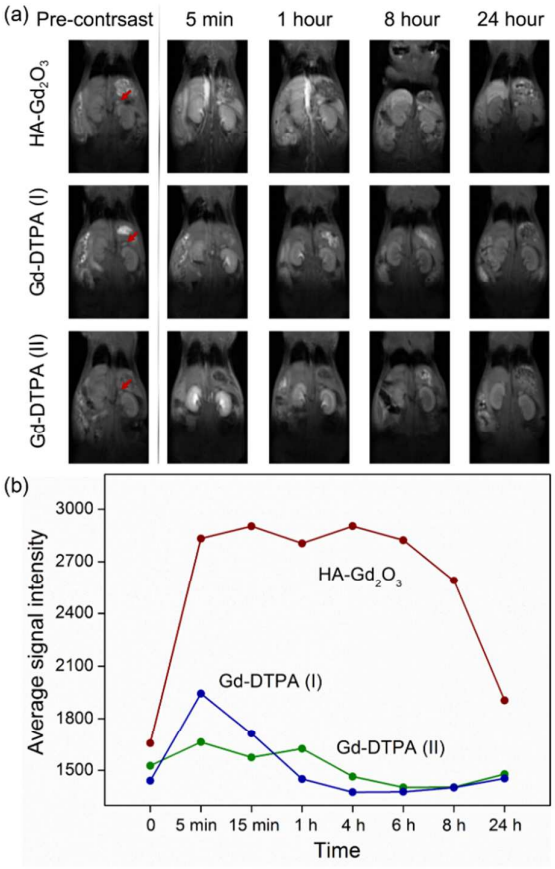

Fig. 5 (a) T_1-weighted MR images of mice after injection of HA-Gd_2O_3 nanoprobe, Gd-DTPA(I): 0.025 mmol Gd/kg and Gd-DTPA(II): 0.1 mmol Gd/kg; Red arrows indicate the regions of adrenal gland; (b) Average signal intensity of adrenal gland of mice with various treatment at different time points.

MR imaging in vivo

Encouraged by the excellent biocompatibility in vitro and in vivo and high r_1 value, MR imaging of mice using the proposed nanoprobe was investigated. As shown in Fig. 5a, after injection of HA-Gd_2O_3 nanoprobe (200 µL, 0.025 mmol/kg) at a quarter of dose in clinical use, MR images showed a rapidly vessels signal enhancement, meanwhile major organs including spleen, liver and kidney became brighter with excellent contrast result 5 min later. At 1 h post injection, the vessels showed the strongest MR signal, the long blood circulation indicated that the nanoprobe could be used as a good contrast agent for blood pool imaging, and the signal in liver and spleen kept the strong intensity, while the MR image of kidney became darker. Like most reported nanoprobes, HA-Gd_2O_3 nanoprobe were mainly accumulated in liver and spleen containing RES system, which revealed that the nanoprobe was mainly metabolized in liver at last. At 24 h post injection, the MR signal in whole body became much weaker, which indicated the probe was mostly metabolized.

Organ-targeted MR imaging plays a crucial role in the diagnosis of various organ morphology-associated diseases.[27, 35] However, the fabrication of organs besides liver and kidney targeted contrast agents was more difficult than that of tumor targeted ones due to the lack of specific interaction between the ligands and receptors. Fortunately, the adrenal gland-targeted ability was found in our developed nanoprobe. As shown in Fig. 5a, the adrenal gland also showed a remarkable signal enhancement at 5 min post injection of nanoprobe, and the strong signal didn't decrease until after 6 h (Fig. S9). That means HA-Gd_2O_3 nanoprobe possessed a specific ability for adrenal gland MR imaging. The mechanism of this phenomenon is not clear, and other HA modified nanoparticles did not show adrenal gland specific imaging. The targeting ability maybe associated with the physical and chemical properties of HA-Gd_2O_3 nanoprobe and some unclearly specific ingestion of adrenal gland, which needs further investigation in the aspect of molecular biology. MR imaging of mice using Gd-DTPA was also performed for the comparison. As shown in Fig. 5b, at 5 min post injection of Gd-DTPA (200 μL, 0.025 mmol Gd/kg), MR images showed a rapidly signal enhancing in liver and kidney after injection and a fast excretion through urine subsequently. Even when the mice were treated with clinic-used dose of Gd-DTPA (200 μL, 0.1 mmol Gd/kg), there were no noticeable improvement for the blood circulation time. At 1 h post injection, the signal in whole body declined obviously, which indicated that most of Gd-DTPA had been cleared from the body. In addition, there were no obvious signal enhancement in adrenal gland with both low and high dosage of Gd-DTPA. The above results further revealed HA-Gd_2O_3 nanoprobe owned the merits of high sensitivity and organ-targeted ability.

Conclusion

In a word, we used HA as template to synthesis a highly sensitive HA-Gd_2O_3 nanoprobe with good biocompatibility by a facile one-pot reaction at room temperature successfully. Based on the SBM theory, HA facilitated the increase of the number and percentage of effective Gd^{3+} in one particle, and the extension of the rotational tumbling time (τ_R) of inner sphere water molecule. The synergistic effects efficiently improved the r_1 value of HA-Gd_2O_3 nanoprobe. In addition, HA as a human inherent molecule insured the excellent biocompatibility of HA-Gd_2O_3 nanoprobe. As a result, the HA-Gd_2O_3 nanoprobe has higher r_1 values, long blood circulation time and excellent biocompatibility in vitro and in vivo. In addition, the proposed nanoprobe shows an obvious organ targeting ability, and could be used for adrenal gland MR imaging in vivo, which showed great potential application in evaluating the morphology of adrenal gland or other adrenal gland disease. More important, the proposed method provide a new strategy for the design of high sensitive and biocompatible MR nanoprobes towards the clinical application.

Acknowledgements

This work was supported by the National Natural Science Foundation of China (Grants 21405112, 21435001), China Postdoctoral Science Foundation (Grants 2014M550146).

Notes and references

1. S. Aime, M. Botta, M. Fasano and E. Terreno, *Chem. Soc. Rev.*, 1998, **27**, 19-29.
2. P. Caravan, J. J. Ellison, T. J. McMurry and R. B. Lauffer, *Chem. Rev.*, 1999, **99**, 2293-2352.
3. Y. Liu and N. Zhang, *Biomaterials.*, 2012, **33**, 5363-5375.
4. K. N. Raymond and V. C. Pierre, *Bioconjug Chem.*, 2005, **16**, 3-8.
5. J. Kim, Y. Piao and T. Hyeon, *Chem. Soc. Rev.*, 2009, **38**, 372-390.
6. D. E. Lee, H. Koo, I. C. Sun, J. H. Ryu, K. Kim and I. C. Kwon, *Chem. Soc. Rev.*, 2012, **41**, 2656-2672.
7. P. P. Adiseshaiah, J. B. Hall and S. E. McNeil, *WIREs Nanomed. Nanobiotechnol*, 2010, **2**, 99-112.
8. A. M. Nystrom and B. Fadeel, *J. Control. Release.*, 2012, **161**, 403-408.
9. A. Dhawan and V. Sharma, *Anal. Bioanal. Chem.*, 2010, **398**, 589-605.
10. J. Ai, E. Biazar, M. Jafarpour, M. Montazeri, A. Majdi, S. Aminifard, M. Zafari, H. R. Akbari and H. G. Rad, *Int. J. Nanomedicine*, 2011, **6**, 1117-1127.
11. E. Terreno, D. D. Castelli, A. Viale and S. Aime, *Chem. Rev.*, 2010, **110**, 3019-3042.
12. P. Caravan, *Chem. Soc. Rev.*, 2006, **35**, 512-523.
13. E. L. Que and C. J. Chang, *Chem. Soc. Rev.*, 2010, **39**, 51-60.
14. G.-L. Davies, I. Kramberger and J. J. Davis, *Chem. Commun.*, 2013, **49**, 9704-9721.
15. F. Chen, W. B. Bu, S. J. Zhang, X. H. Liu, J. N. Liu, H. Y. Xing, Q. F. Xiao, L. P. Zhou, W. J. Peng, L. Z. Wang and J. L. Shi, *Adv. Funct. Mater.*, 2011, **21**, 4285-4294.
16. J. Y. Park, M. J. Baek, E. S. Choi, S. Woo, J. H. Kim, T. J. Kim, J. C. Jung, K. S. Chae, Y. Chang and G. H. Lee, *ACS Nano*, 2009, **3**, 3663-3669.
17. H. Otsuka, Y. Nagasaki and K. Kataoka, *Adv. Drug Deliver. Rev.*, 2012, **64**, 246-255.
18. N. Ma, A. F. Marshall and J. H. Rao, *J. Am. Chem. Soc.*, 2010, **132**, 6884-6885.
19. J. P. Xie, Y. G. Zheng and J. Y. Ying, *J. Am. Chem. Soc.*, 2009, **131**, 888-889.
20. C. L. Guo and J. Irudayaraj, *Anal. Chem.*, 2011, **83**, 2883-2889.
21. P. Wu, T. Zhao, Y. Tian, L. Wu and X. Hou, *Chem. Eur. J.*, 2013, **19**, 7473-7479.
22. B. Zhang, H. Jin, Y. Li, B. Chen, S. Liu and D. Shi, *J. Mater. Chem.*, 2012, **22**, 14494-14501.
23. S.-K. Sun, L.-X. Dong, Y. Cao, H.-R. Sun and X.-P. Yan, *Anal. Chem.*, 2013, **85**, 8436-8441.
24. C. I. Richards, S. Choi, J. C. Hsiang, Y. Antoku, T. Vosch, A. Bongiorno, Y. L. Tzeng and R. M. Dickson, *J. Am. Chem. Soc.*, 2008, **130**, 5038-5039.

25. B. P. Toole, *Nat. Rev. Cancer*, 2004, **4**, 528-539.
26. H.-J. Cho, H. Y. Yoon, H. Koo, S.-H. Ko, J.-S. Shim, J.-H. Cho, J. H. Park, K. Kim, I. C. Kwon and D.-D. Kim, *J. Control. Release*, 2012, **162**, 111-118.
27. M. Moon, R. Thomas, S.-u. Heo, M.-S. Park, W. Bae, S. Heo, N. Yim and Y. Jeong, *Mol. Imaging Biol.*, 2015, 1-7.
28. T. V. Anilkumar, J. Muhamed, A. Jose, A. Jyothi, P. V. Mohanan and L. K. Krishnan, *Biologicals.*, 2011, **39**, 81-88.
29. E. K. Lim, H. O. Kim, E. Jang, J. Park, K. Lee, J. S. Suh, Y. M. Huh and S. Haam, *Biomaterials.*, 2011, **32**, 7941-7950.
30. M. Yu, S. Jambhrunkar, P. Thorn, J. Chen, W. Gu and C. Yu, *Nanoscale*, 2013, **5**, 178-183.
31. F. Söderlind, H. Pedersen, R. M. Petoral Jr, P.-O. Käll and K. Uvdal, *J. Colloid Interf. Sci.*, 2005, **288**, 140-148.
32. D. Raiser and J. P. Deville, *J. Electron Spectrosc*, 1991, **57**, 91-97.
33. A. T. M. Anishur Rahman, K. Vasilev and P. Majewski, *J. Colloid Interf. Sci.*, 2011, **354**, 592-596.
34. Y. Yang, Y. Sun, Y. Liu, J. Peng, Y. Wu, Y. Zhang, W. Feng and F. Li, *Biomaterials.*, 2013, **34**, 508-515.
35. C. J. Sun, H. Yang, Y. Yuan, X. Tian, L. M. Wang, Y. Guo, L. Xu, J. L. Lei, N. Gao, G. J. Anderson, X. J. Liang, C. Y. Chen, Y. L. Zhao and G. J. Nie, *J. Am. Chem. Soc.*, 2011, **133**, 8617-8624.